Improved Control of Three Phase Dual-Stage Grid-Connected PV System Based on a Predictive Control Strategy

Abdelbaset Laib, Fateh Krim, Billel Talbi, Abbes Kihal, Hamza Feroura

LEPCI Laboratory, Electronics Dept, University of Setif 1, Route de Béjaïa, 19000, Sétif, Algeria
(Tel: +213777159128; e-mail: laib_abdelbaset@univ-setif.dz).

Abstract: This paper focuses on the control of three phase dual-stage grid connected photovoltaic (PV) system. The control objective is to generate the maximum power from PV arrays under irradiation changes and transfer it into the grid, in addition to the reactive power demanded by the grid operator while providing high grid current quality. A quick and accurate control method based on variable step size incremental conductance and predictive current control (VS-INC/PCC) is proposed and applied to the first stage (DC-DC Boost converter) in order to achieve a quick maximum power point tracking MPPT with less power oscillations. Furthermore, a voltage-oriented control based on both predictive control strategy and space vector modulation SVM (PS-VOC) is applied to the second stage (Two-level inverter) whose objective is to control the d-q axis grid currents. The proposed system is simulated using Matlab/Simulink and Simpower packages. As results, the proposed MPPT provides a quick and accurate tracking with significant oscillation reduction at the MPP under irradiation changes in comparison with the conventional methods. Besides, the injection of the extracted PV power and the reactive power demanded by the grid operator are provided with high current quality due to the capability of the proposed PS-VOC control method.

Keywords: Photovoltaic energy, dual-stage grid-connected PV system, maximum power point tracking (MPPT), predictive control strategy, d-q axis grid currents control.

1. INTRODUCTION

During the last years, photovoltaic (PV) energy has attracted a substantial attention to overcome the increased energy consumption and environmental problems (pollution, global warming …etc) (Wai et al., 2008). Grid connected PV systems have been used to inject the power from the PV arrays into the public grid (Bratcu et al., 2008; Ahmed et al., 2013; de Oliveira et al., 2016; Menadi et al., 2015). The present challenge is to extract the maximum power from the PV arrays and deliver it to the grid with high current quality under climatic changes. For this reason, many research works exist on these challenges for two grid PV system topologies namely single and dual stage (Ahmed et al., 2013; Chen et al., 2014). The latter topology is frequently used due to the fact that MPPT and control of the power injected into the grid are decoupled by means of two different converters. This advantage eases the MPP tracking as well as boosts the DC-link voltage value above the grid peak voltage value whatever the produced power (Ahmed et al., 2013).

PV arrays still do not provide a maximum efficiency, since their performance depends on climatic conditions. The random changes of these conditions reduce the PV array output power. For this reason, numerous MPPT techniques existing in the literature can be employed to control the first stage (DC-DC boost converter) in order to force the PV systems to continuously pursuing and rapidly extracting the maximum power from PV arrays. Among these techniques, conventional MPPT techniques such as perturb and observe

(P&O) (Azzouzi, 2013) or Incremental conductance (INC) (Safari and Mekhilef, 2011) have been intensively investigated in the last decade (Bendib et al., 2015). Nevertheless, these techniques present three major drawbacks: loss of tracking direction, low tracking speed and large oscillations. Recently, several intelligent techniques such as fuzzy logic (Zainuri et al., 2013; Radjai et al., 2014; Algazar et al., 2012), neural networks (Boumaaraf et al., 2015), genetic algorithms (Harrag and Messalti, 2015) and particle swarm optimisation (de Oliveira et al., 2016), have been introduced in order to enhance the performance. However, it is still difficult to implement them practically. In addition, due to the implementation simplicity of the conventional MPPT algorithms, other control schemes based on these algorithms have been proposed to improve the efficiency of PV arrays by including an internal voltage loop as MPPT voltage-oriented loop (Pradhan et al., 2016; Kakosimos et al., 2013, Kihel et al., 2017) or an internal current loop as MPPT current oriented loop (Bianconi et al., 2013; Kakosimos et al., 2013). These latter afford an accurate MPP tracking as well as a satisfactory oscillation reduction at the MPP, owing to the linear relation between the PV array current and solar irradiation. Numerous current controllers are employed in MPPT current oriented loop method such as PI controller (Kollimalla and Mishra, 2014), predictive controller (Kakosimos et al., 2013), finite set predictive controller (Kakosimos and Kladas, 2011; Talbi et al., 2017, Talbi et al., 2018) and sliding mode controller (Bianconi et al., 2013). Predictive current controller offers significant advantages such as implementation simplicity and high-

performance regarding response time and PV current ripple compared to PI controller. Moreover, it has fixed frequency unlike to sliding mode and finite set predictive controllers.

In this paper, the control of three phase dual-stage grid connected PV system is proposed. The first stage is the MPPT controller. In order to improve the performance in terms of MPP tracking accuracy, dynamic response speed and oscillation reduction at the MPP, a variable incremental current step size of an MPPT current oriented loop based on predictive current control for this stage is proposed as the first part in this contribution.

The role of the second stage is to inject the extracted PV power into the grid with a high grid current quality. For this purpose, numerous control techniques are proposed. Among them, control methods without modulation stage such as: grid current control based on hysteresis controllers (Jain and Singh, 2017), finite set model predictive control strategy (Rodriguez et al., 2007, Feroura et al., 2017a, Feroura et al., 2017b), direct power control DPC based on switching table (Hu and Zhu, 2011). All these techniques provide a high performance. However, they have a variable inherent switching frequency, which is a major disadvantage. On the other hand, control methods with modulation stage such as: voltage-oriented control (VOC) (Teodorescu et al., 2011), voltage-based direct power control (V-DPC) (Mariusz Malinowski et al., 2004), virtual flux-oriented control (VFOC) (Malinowski et al., 2001) are based on PI regulators in internal current control loop in addition to modulation stage (PWM or SVM). These techniques operate with a fixed switching frequency. However, the slow regulation of PI regulators and control delay deteriorate the performance.

So, as a second contribution in this paper, for the second stage control, a predictive control strategy is integrated to control VOC based on synchronous frame (d-q), in order to eliminate the PI regulators drawbacks as well as the control delay under PV power injection into the grid with a high quality.

The proposed global system, including the two stages, is simulated using Matlab/Simulink and simpower packages, where different tests are carried out in order to check the system performance. Similarly, a comparison in terms of oscillations, tracking accuracy and response time is performed between the proposed and conventional MPPT methods. Meanwhile, the i_d-i_q currents control and grid current quality are observed and evaluated under irradiation and reactive power reference changes.
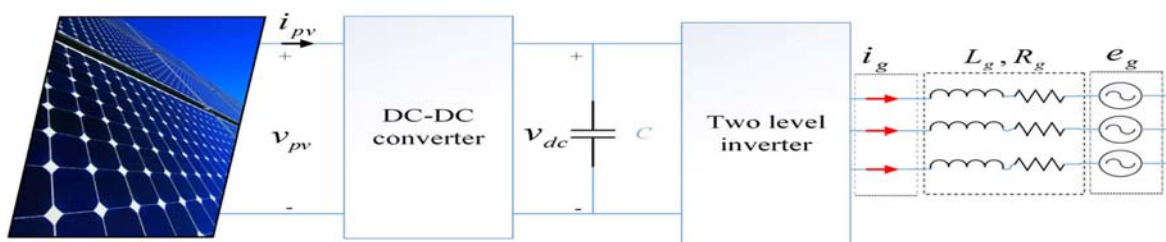
The remainder of this paper is arranged as follows. The second section introduces the configuration and control scheme of the proposed system. Simulation results and discussions are presented in the third section, after which conclusions are drawn in the final section.

2. GLOBAL SYSTEM CONFIGURATION AND CONTROL

The global system mainly consists of: PV array, DC-DC converter (boost), two-level inverter, and R_g, L_g filter tied to grid, as shown in Fig. 1.

The PV array behaves like current generator with variable I(V) current characteristic (Petcut and Leonida-Dragomir, 2010), where it converts solar radiation into electrical power.

The role of the boost converter is to track the MPP and deliver it continuously to the DC-link. The two-level inverter injects the power coming from the DC-DC boost into the grid considering the grid current quality.

As shown in Fig. 2, the global system is controlled by three controllers:

A) VS-INC/PCC controller whose role is to track the MPP quickly and accurately.

B) PI controller to regulate the DC-link voltage.

C) PS-VOC controller for i_d-i_q grid currents.

2.1 Proposed MPPT control

Under irradiation changes, the extreme current I_{mpp} must be tracked quickly with less ripple to reach the maximum power P_{mpp}. In this paper, an MPPT method based on the combination of both conventional current incremental algorithm (Kakosimos et al., 2011) and variable step size algorithm (Liu et al., 2008; Loukriz and al., 2016) is considered.

Variable Current Step Size Incremental Algorithm

The current incremental algorithm as the conventional method is based on the slope of the PV power curve (Safari and Mekhilef, 2011). It identifies the instantaneous position value to the maximum power point; zero at the MPP, negative on the left-hand side of the MPP and positive on the right-hand side of the MPP; i_{ref} increases when the slope is positive and decreases when it is negative.

Fig. 1. Global System Configuration.
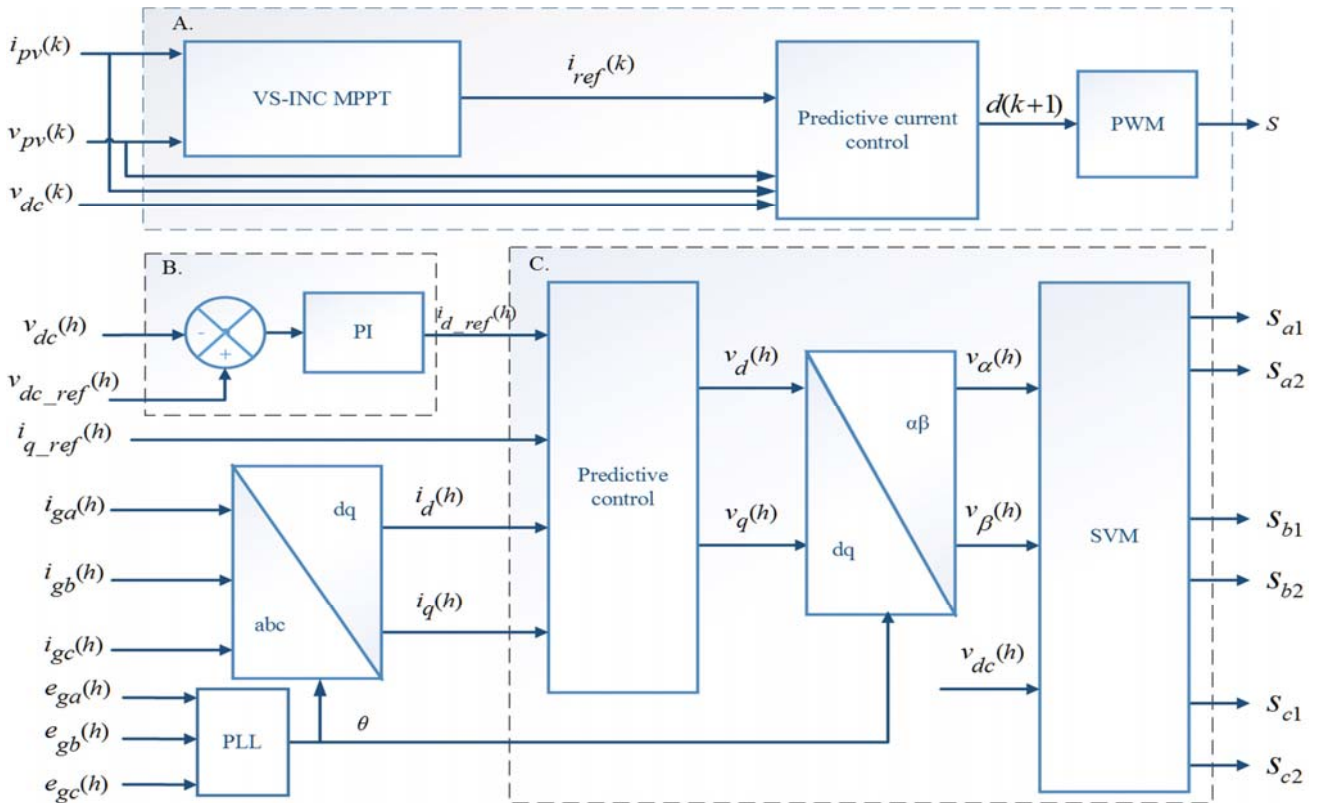
Fig. 2. Global System Control (A) proposed MPPT controller (B) DC-link voltage controller (C) proposed PS-VOC controller.

The basic equations of this method are as follows

$$\frac{dp_{pv}}{di_{pv}} = 0 \tag{1}$$

Equation (1) can be expressed as

$$\frac{dp_{pv}}{di_{pv}} = \frac{d(v_{pv} * i_{pv})}{di_{pv}} = \frac{dv_{pv}}{di_{pv}} i_{pv} + v_{pv} \tag{2}$$

$$\frac{dv_{pv}}{di_{pv}} > -\frac{v_{pv}}{i_{pv}} \qquad \text{at right of the MPP} \tag{3}$$

$$\frac{dv_{pv}}{di_{pv}} < -\frac{v_{pv}}{i_{pv}} \qquad \text{at left of the MPP} \tag{4}$$

$$\frac{dv_{pv}}{di_{pv}} = -\frac{v_{pv}}{i_{pv}} \qquad \text{at the MPP} \tag{5}$$

The proposed MPPT scheme is employed with an algorithm of variable current step size, which is added to the current INC in order to obtain an enhancement in terms of response time and oscillation at the MPP. A small positive quantity e is considered in order to separate the dynamic and steady states tracking operation. In addition, the calculation of the ratio M is given by (6); when M is bigger than the chosen positive value e, the step Δi_{ref} takes a big value as well as the MPP will be reached quickly. Thus, when it is smaller than e, Δi_{ref}

will take a small value and consequently, the power oscillation at the MPP will be reduced.

$$M = \left| \frac{\Delta p_{pv}}{\Delta v_{pv}} \right| \tag{6}$$

From Fig. 3, it is clear that the ratio M takes large positive value in case where the PV power point is far left or far right from the MPP. In contrast, when PV power is close to the MPP, M takes very small positive value. For this reason, the value e is chosen as small positive value in order to separate the steady and dynamic states tracking.
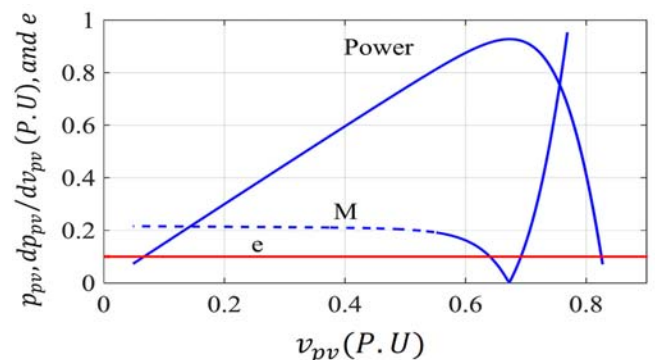
Fig. 3. Basic idea of VS-INC current algorithm on P-V curve.

Fig. 4 represents the flowchart of the proposed current MPPT algorithm.
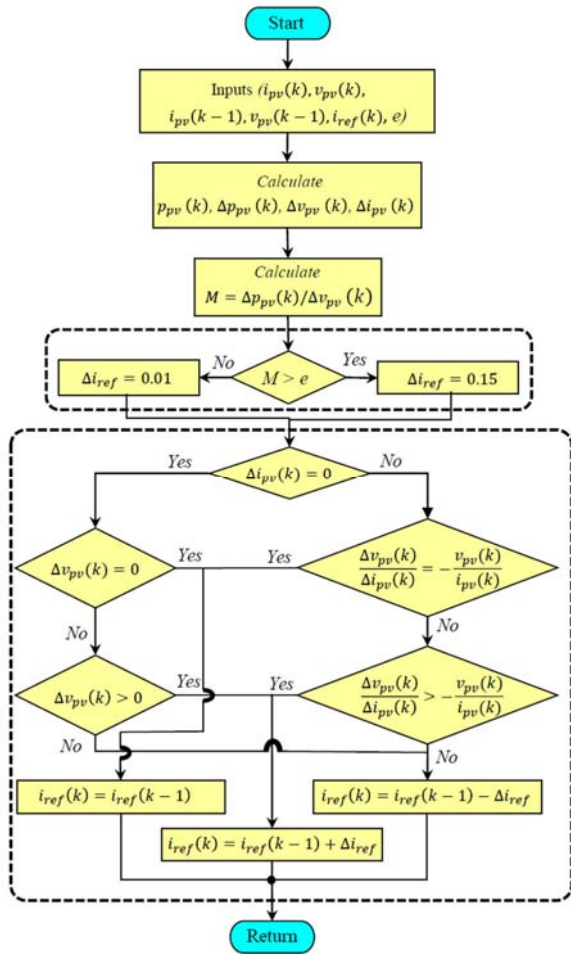
Fig. 4. Flowchart of the VS-INC current MPPT.

Predictive current control

The role of the predictive current controller is to enforce i_{pv} to track i_{ref} delivered by the MPPT unit via control of the DC-DC boost converter using predicted duty cycle. The determination of the predicted duty cycle is based on exact knowledge of DC-DC boost converter model (Kakosimos et al., 2013). Fig. 5 illustrates the equivalent circuit of DC-DC boost converter considering ON and OFF switching states.

When the switch is ON (Fig. 5 (a)), the boost converter equations can be described as follows

$$\begin{cases} L\dfrac{di_{pv}(t)}{dt} = v_{pv}(t) \\ C\dfrac{dv_{dc}(t)}{dt} = -i_{inv}(t) \end{cases} \quad (7)$$

When the switch is OFF (Fig. 5 (b)), the boost converter equations yield

$$\begin{cases} L\dfrac{di_{pv}(t)}{dt} = [v_{pv}(t) - v_{dc}(t)] \\ C\dfrac{dv_{dc}(t)}{dt} = [i_{pv}(t) - i_{inv}(t)] \end{cases} \quad (8)$$
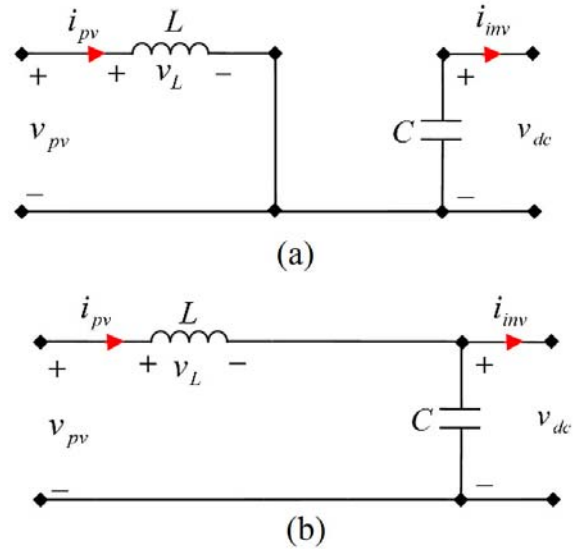
Fig. 5. DC-DC equivalent circuit.

The averaged system (9) of the systems (7) and (8) over a switching period T_p is obtained by multiplying (7) and (8) by the duty cycle $d(t)$ and $1-d(t)$ respectively (Van Dijk et al., 1995).

$$\begin{cases} L\dfrac{di_{pv}(t)}{dt} = v_{pv}(t) - v_{dc}(t) + v_{dc}(t)d(t) \\ C\dfrac{dv_{dc}(t)}{dt} = i_{pv}(t) - i_{inv}(t) - i_{pv}(t)d(t) \end{cases} \quad (9)$$

By applying Euler's discretization rule and considering the switching period T_p the discrete time system of (9) is given as follows (Kakosimos et al., 2013)

$$\begin{cases} i_{pv}(k+1) = i_{pv}(k) + \dfrac{T_p}{L}[v_{pv}(k) + (d(k)-1)v_{dc}(k)] \\ v_{dc}(k+1) = v_{dc}(k) + \dfrac{T_p}{C}[(1-d(k))i_{pv}(k) - i_{inv}(k)] \end{cases} \quad (10)$$

In order to obtain duty cycle at instant k+1, system (10) is extended for one switching period and can be rewritten as

$$i_{pv}(k+2) = i_{pv}(k+1) + \frac{T_p}{L}[v_{pv}(k+1) + (d(k+1)-1)v_{dc}(k+1)] \quad (11)$$

To solve system (11), we assume that the current i_{pv} is regulated at its reference i_{ref} delivered by MPPT unit (Kakosimos et al., 2013) which means

$$i_{pv}(k+2) = i_{ref}(k+2) \quad (12)$$

And for sufficiently small sampling period T_p, it can be assumed that $i_{ref}(k+2) = i_{ref}(k)$ and no extrapolation is needed.

Assumed that v_{pv} and v_{dc} do not change considerably during one switching period and, thus $v_{pv}(k+1)$ and $v_{dc}(k+1)$ can be estimated as

$$\begin{cases} v_{pv}(k+1) = v_{pv}(k) \\ v_{dc}(k+1) = v_{dc}(k) \end{cases} \tag{13}$$

From (11), (12) and (13), the predicted duty cycle for the next sampling period can be derived as

$$d(k+1) = \frac{\dfrac{L}{T_p}[i_{ref}(k) - i_{pv}(k+1)] - v_{pv}(k)}{v_{dc}(k)} + 1 \tag{14}$$

The predicted duty cycle obtained from (14) is compared with a sawtooth waveform signal to generate a modulated PWM signal (*S*) to control the DC-DC boost converter.

2.2 Proposed PS-VOC control

In this section, rotating frame *d-q* grid currents control for the two-level inverter is performed through PS-VOC control strategy. As shown in Fig. 2, this control strategy is based on the calculation of the reference voltage vector which is applied during the next sampling time through SVM modulation in order to minimize the error between the predicted currents $i_d(h+1)$, $i_q(h+1)$ and their respective references $i_{d\_ref}(h+1)$, $i_{q\_ref}(h+1)$. From $i_{d\_ref}(h)$ estimated by DC-link PI controller and $i_{q\_ref}(h)$ estimated according to reactive power demanded by the grid operator (15)

$$i_{q\_ref}(h) = \frac{Q_{ref}(h)}{e_{gd}(h)*1.5} \tag{15}$$

where, e_{gd} is the direct component of grid voltage in d-q frame.

One can easily assume that $i_{d\_ref}(h+1)=i_{d\_ref}(h)$ and $i_{q\_ref}(h+1)=i_{q\_ref}(h)$ and no extrapolation is needed due to sufficiently small sampling period.

To apply predictive control strategy, the grid-tied inverter model is necessary to calculate the voltage vector reference corresponding to the predicted currents. The required mathematical model in natural frame (abc) is described by (Rodriguez et al., 2007)

$$\frac{di_g(t)}{dt} = \frac{1}{L_g}[v(t) - e_g(t) - R_g i_g(t)] \tag{16}$$

where v, e_g and i_g are voltage vectors generated by the inverter, grid voltages and grid currents respectively.

From (16), the grid tied inverter model in rotating frame *d-q* can be expressed as follows (Yaramasu et al., 2014)

$$\begin{cases} \dfrac{di_d(t)}{dt} - \omega_g i_q(t) = \dfrac{1}{L_g}[-R_g i_d(t) - e_d(t) + v_d(t)] \\ \dfrac{di_q(t)}{dt} + \omega_g i_d(t) = \dfrac{1}{L_g}[-R_g i_q(t) - e_q(t) + v_q(t)] \end{cases} \tag{17}$$

where ω_g is the grid angular frequency.

Euler forward method is used to approximate the derivatives in (17) in order to obtain the discrete time model,

$$\begin{cases} \dfrac{di_d(t)}{dt} = \dfrac{i_d(h+1) - i_d(h)}{T_m} \\ \dfrac{di_q(t)}{dt} = \dfrac{i_q(h+1) - i_q(h)}{T_m} \end{cases} \tag{18}$$

where T_m is the sampling period.

The discrete time model of (17) can be described by (19)

$$\begin{cases} i_d(h+1) = \dfrac{T_m}{L_g}[-R_g i_d(h) - e_d(h) + v_d(h)] + T_m \omega_g i_q(h) + i_d(h) \\ i_q(h+1) = \dfrac{T_m}{L_g}[-R_g i_q(h) - e_q(h) + v_q(h)] - T_m \omega_g i_d(h) + i_q(h) \end{cases} \tag{19}$$

To calculate the reference voltage vector ($v_d(h)$ $v_q(h)$) that can be given to SVM modulator, the predicted i_d-i_q synchronous frame currents should track their respective references i_{d_ref}-i_{q_ref} during the next sampling time, which means

$$\begin{cases} i_d(h+1) = i_{d\_ref}(h) \\ i_q(h+1) = i_{q\_ref}(h) \end{cases} \tag{20}$$

By substituting (20) in (19), the reference voltage vector can be expressed as

$$\begin{cases} v_d(h) = \dfrac{L_g}{T_m}(i_{d\_ref}(h) - i_d(h)) + R_g i_d(h) + e_d(h) - \omega_g L_g i_q(h) \\ v_q(h) = \dfrac{L_g}{T_m}(i_{q\_ref}(h) - i_q(h)) + R_g i_q(h) + e_q(h) + \omega_g L_g i_d(h) \end{cases} \tag{21}$$

The obtained reference voltage vector ($v_d(h)$, $v_q(h)$) by (21) is transferred to αβ frame and applied during the next sampling time through SVM modulation.

3. RESULTS AND DISCUSSION

In order to evaluate the proposed control scheme performance illustrated in Fig. 2, extensive simulations with the specifications depicted in Table 1 are performed for the global system presented in Fig. 1 using MATLAB/Simulink and simpower packages. The core of the VS-INC, PCC and PS-VOC algorithms are implemented using embedded

MATLAB functions as program lines. Moreover, the power converters are built by simpower system toolbox components. The PV array characteristics namely P(V), I(V) used in the simulation are shown in Fig. 6. Fig. 7 depicts simulation model of the proposed control scheme for dual-stage grid-connected PV system in Simulink environment.

Table 1. Global system parameters.

PV Siemens SM110 electrical parameters	Value
Maximum power ($Pmpp$)	110 W
Open circuit voltage (Voc)	43.5 V
Short circuit current (Isc)	3.45 A
Voltage at Pmax	35 V
Current at Pmax	3.15 A
Number of cells connected in parallel (Np)	1
Number of cells connected in series (Ns)	72
Number of modules connected in series (Nss)	2
Number of modules connected in parallel (Npp)	2
Boost converter electrical parameters	**Value**
Resistor R	50 Ω
Inductor L	40 mH
Capacitor C	1100μF
Grid electrical parameters	**Value**
Grid inductance Lg	10 mH
Grid resistance Rg	0.1 Ω
Grid Voltage e_g	50 V
Grid frequency Fg	50 Hz
Simulation parameters	**Value**
MPPT sampling time Ts	1 ms
SVM sampling period Tm	5 ms
PWM switching period Tp	5 ms

This section is divided into two parts. In the first part, the objective is to compare the proposed MPPT (VS-INC/PCC) with both INC/PCC and conventional INC in terms of MPP tracking speed, accuracy and power oscillations under solar irradiation changes. In the second part, the objective is to test the effectiveness of the proposed PS-VOC control technique regarding i_d-i_q grid current regulation and grid current quality under irradiation changes and also reactive power demanded by the grid operator changes.

3.1 VS-INC/PCC versus INC/PCC and conventional INC comparisons

Under irradiation changes represented in Fig. 8(a), the proposed VS-INC/PCC MPPT method, INC/PCC, and conventional INC are tested by numerical simulation. Initially, the irradiance level is set to 500 W/m². Then, at 0.1 s, a sudden irradiation change from 500 to 700 W/m² occurs. With VS-INC/PCC method MPP is reached after 7 ms, while with INC/PCC it takes 18 ms. As the conventional method reaches the MPP during 34 ms with tracking direction drift. Then the irradiation level is decreased slowly from 700 to 400 W/m² during a time interval of 0.2 s. The proposed method exhibits better accuracy tracking than both INC/PCC and conventional INC as shown in Fig. 8.
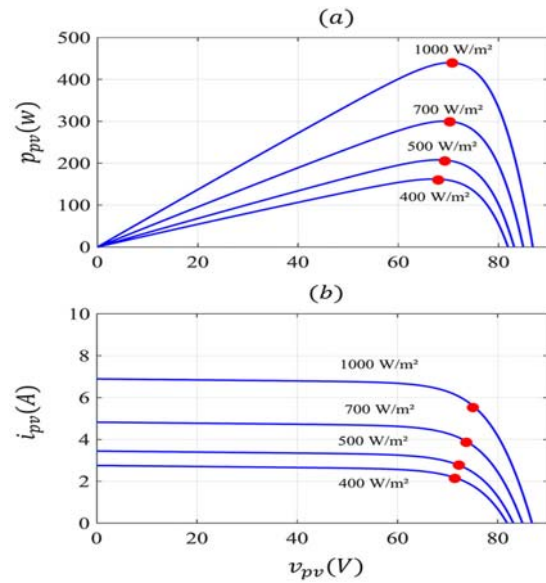
Fig. 6. PV system characteristics: (a) P (V); (b) I (V).

Finally, a sudden irradiation change from 400 to 1000 W/m2 occurs at 0.5 s, the improved MPPT shows also a faster tracking than both INC/PCC and conventional MPPT, where the proposed MPPT takes only 25 ms to reach the MPP while the INC/PCC needs 56 ms and conventional MPPT needs 100 ms as shown in Fig. 8(d).

On other side, the proposed MPPT shows a high performance in term of power oscillation compared to INC/PCC and conventional methods as depicted in Fig. 9, where the oscillation widths around MPPs, by using the proposed method, under different steady irradiations levels (500, 700, 400 and 1000 W/m²) are [209.2- 209.7], [301.6- 302], [163.4-163.8], and [439.8- 440] respectively. In counterpart, the widths of power oscillation widths by using the INC/PCC method are [208.5- 209.7], [300.5- 302], [162.2- 163.8], [440- 439.4] respectively, and when using the conventional one they are [206- 209.7], [299- 302], [161- 163.8], [437.2-440] respectively.

Table 2 summarized the comparison between the proposed VS-INC/PCC MPPT method, INC/PCC, and conventional INC in terms of MPPT tracking speed, accuracy and power oscillations.

As shown in simulations results, the MPPT algorithms based on predictive current control respond to the change in irradiation quickly and accurately than the conventional algorithm, due to the linear relationship between the irradiance and the PV current (Bianconi et al., 2013). This linear relationship demonstrates that it's a beneficial factor toward the MPP rapidly and accurately. Furthermore, the developed variable step size current Incremental conductance algorithm makes the proposed MPPT scheme quicker and more accurate with a significant power oscillations reduction compared to both conventional algorithms. Where, it provides high Δi_{ref} during sudden irradiations and a small Δi_{ref} for fixed or slow irradiation changes as shown in Fig. 10.
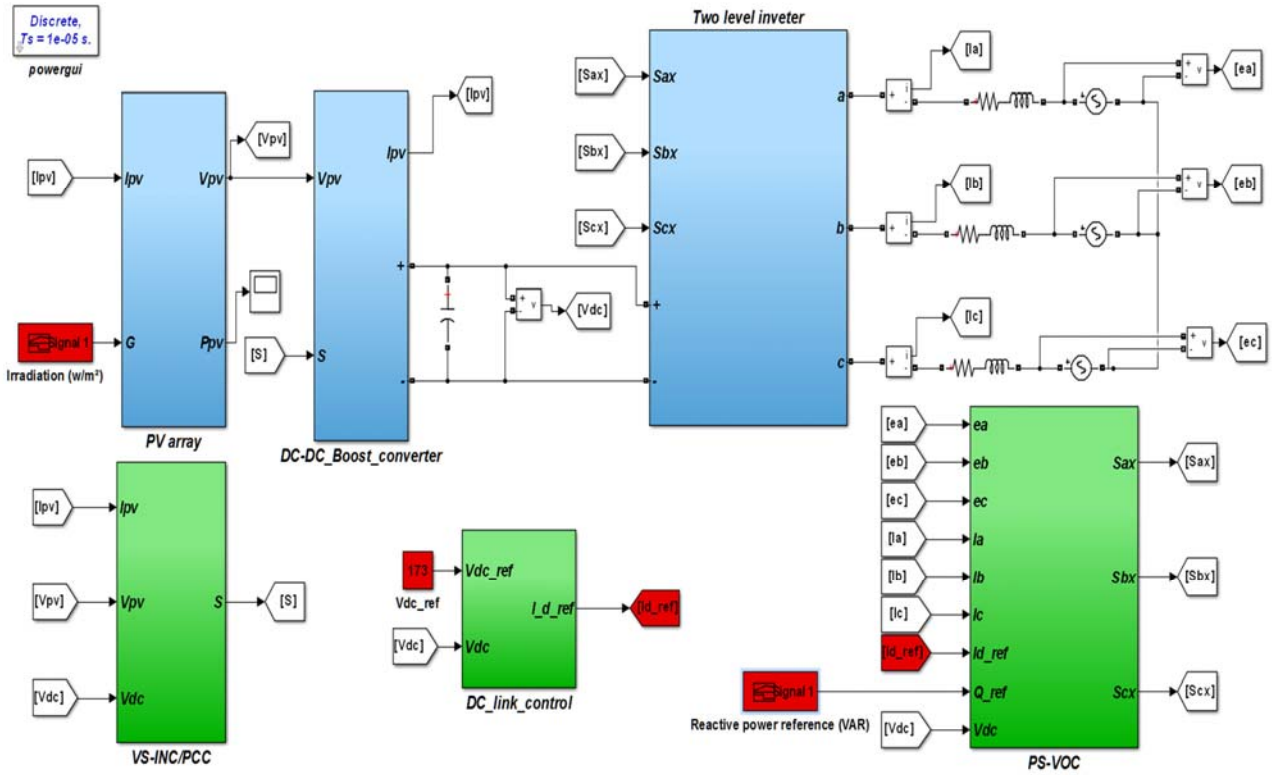
Fig. 7. Simulation block scheme of the proposed control strategy for dual-stage grid-connected PV system.

Table 2. Summary of MPPT simulation results.

Technique	Step change in irradiance 500→700 W/m²		Linear change in irradiance 700→400W/m²	Step change in irradiance 400→1000W/m²	
	Tracking speed time (*ms*)	Power oscillation (*W*)	Tracking accuracy	Tracking speed time (*ms*)	Power oscillation (*W*)
Conventional INC	34	3	Bad (power deviation)	100	2.8
INC/PCC	18	1.5	Good	56	0.6
VS-INC/PCC	7	Less than 0.4	Very Good	25	Less than 0.2

On the other hand, the INC/PCC provides a fixed Δi_{ref} under all irradiation changes.

3.2 Performance of PS-VOC under irradiation changes

This section deals with test of the global system performance under different irradiation changes and presents the efficiency of the applied method in terms of *d-q* currents control and grid current THD.

Firstly, as illustrated in Fig. 11(a), for a fixed irradiation condition at 500 W/m² during the interval [0, 0.1s], the PV array output is oscillating around the MPP and v_{dc} is completely maintained to its reference. Hence, i_d and i_q are

regulated according to their references by means of the proposed method (PS-VOC), as observed in Fig. 11(c, d). Furthermore, the grid currents are balanced and sinusoidal.

Afterward, the sudden irradiation changes from 500 to 700 W/m² at instant 0.1s leads to an increase in the PV power output and a small deviation in v_{dc} from its reference as shown in Fig. 11(a, b). Despite that, i_d and i_q remain tracking their references, whereas the grid currents are increased and kept sinusoidal due to the capability of the proposed method. Then, under the slow irradiation change from 700 to 400 W/m² during the time interval 0.2 to 0.4s, the PV power decreases slowly. Also, v_{dc} is a bit far from its reference as illustrated in Fig. 11(b). Meanwhile, $i_d\_i_q$ currents track their

(a)

(b)

(c)

(d)
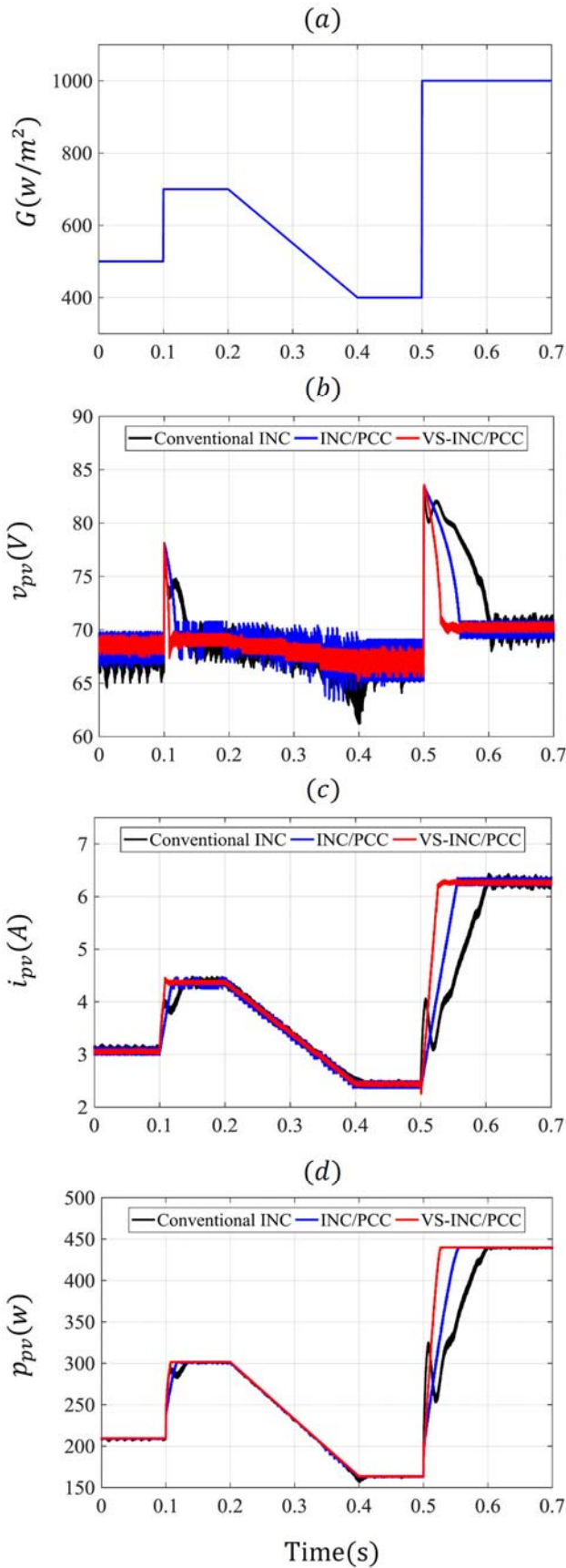
Fig. 8. Performance of INC, INC/PCC and proposed MPPT under irradiation changes.
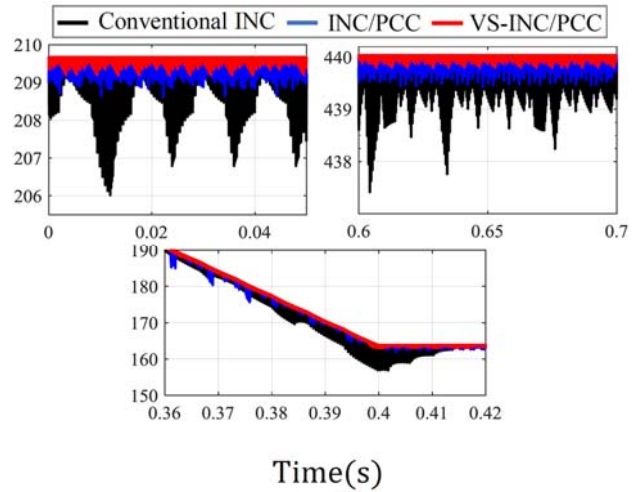
Fig. 9. Zoom of PV power output.
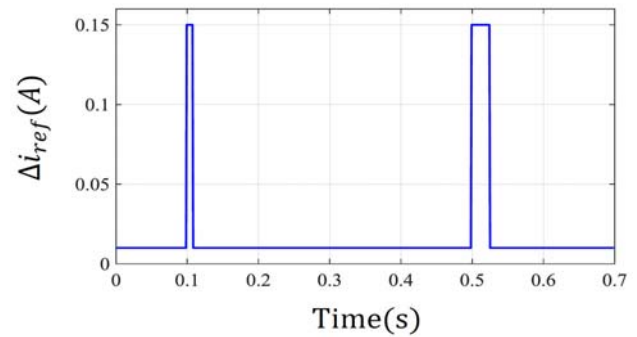
Fig. 10. Behavior of proposed VS-INC.

references and grid currents are decreasing with a sinusoidal form.

Finally, a large sudden change in irradiation occurs at instant 0.5 s. The PV power output is rapidly increased, which leads to a large deviation of v_{dc} from its reference, as shown in Fig. 11(b) even though, i_d and i_q remain tracking their references whereas the grid currents remain sinusoidal. This is due to the efficiency of the proposed method.

As presented in Table 3, the proposed method (VOC based on predictive strategy through SVM) provides high grid current quality under all irradiation change level cases according to the international standards (IEEE-519, THDi< 5%).

Table 3. Obtained THD under different irradiation levels.

Irradiation G(W/m²)	500	700	400	1000
THDi%	3.56	2.66	4.08	1.51

3.3 Performance of PS-VOC under reactive power reference changes

In this section, the performance of the proposed PS-VOC is examined under reactive power reference changes and fixed PV power output at 440 W.

As shown in Fig. 12, the reactive power reference is set to zero during 0.2s, hence, the i_{q_ref} is also set to zero. The DC-link voltage is completely maintained to its reference, when
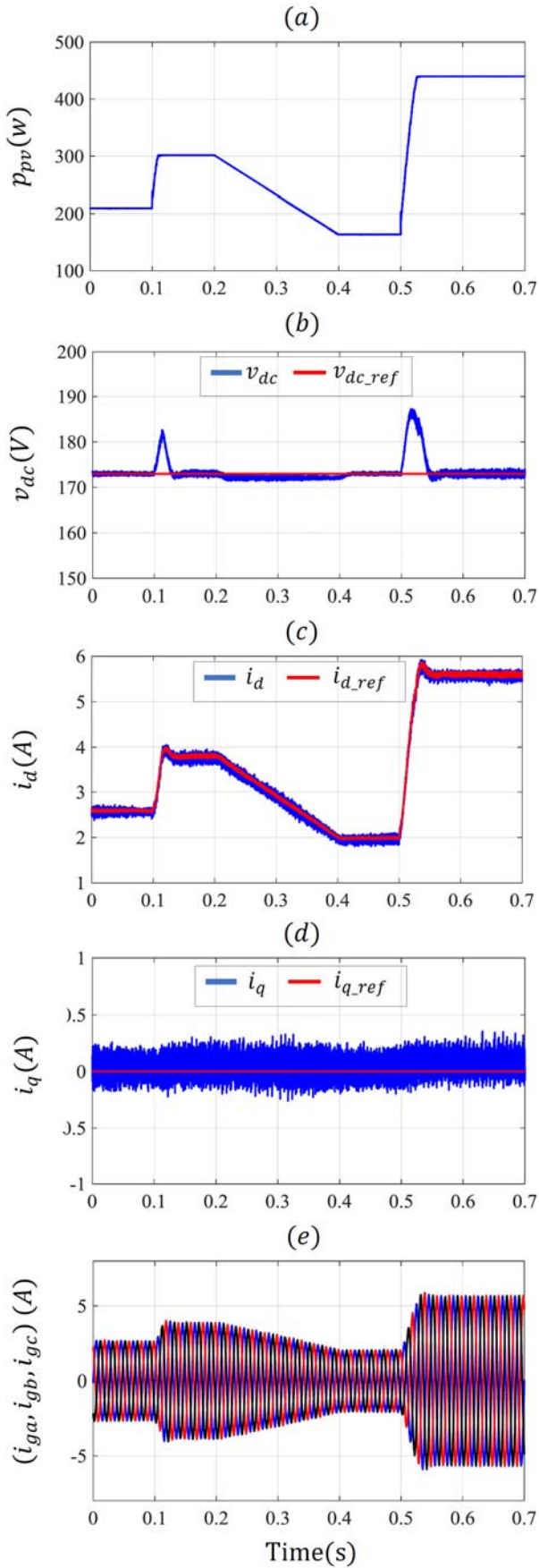
Fig. 11. Performance of global system under irradiation changes.
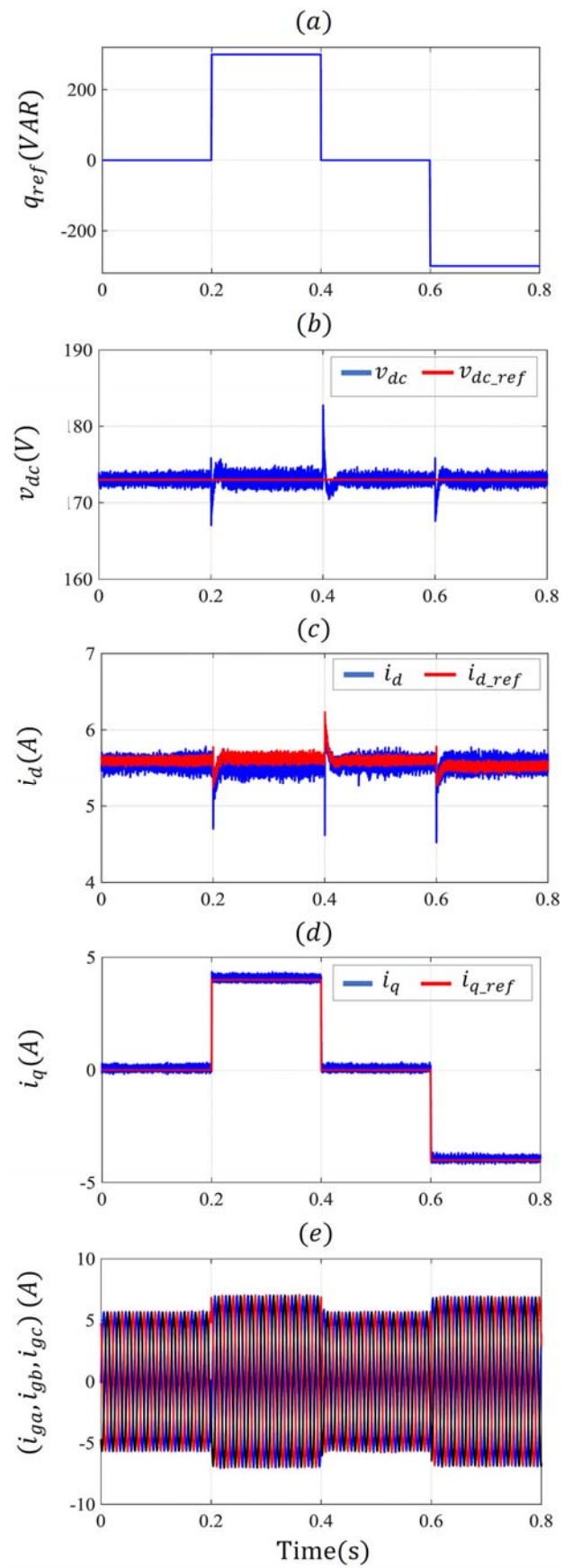
Fig. 12. Performance of global system under reactive power grid operator demand changes.

the i_d-i_q currents track their references and the grid currents are sinusoidal.

Next, at instant 0.2 s, a sudden increase from 0 to 300 VAR is occurred in the reactive power reference while, the i_q reference is estimated to be 4 A. The proposed PS-VOC method shows a rapid i_q tracking to its reference (2.7 ms). Besides, the grid currents increase swiftly due to the increase in grid apparent power Sg, where the grid current amplitude is proportional to Sg. It is also observed that the angle between the grid currents and grid voltage is changed as depicted in Fig. 13(a).

Then, at instant 0.4 s, a sudden decrease from 300 to 0 VAR in the reactive power reference occurs while, i_{q_ref} is set to 0A. The ability of the proposed PS-VOC shows a quick tracking of i_q to its reference (4 ms). Also, grid currents amplitude increase is observed due to the increase of apparent power Sg. While the grid currents and voltages become in phase as illustrated in Fig. 13(b).
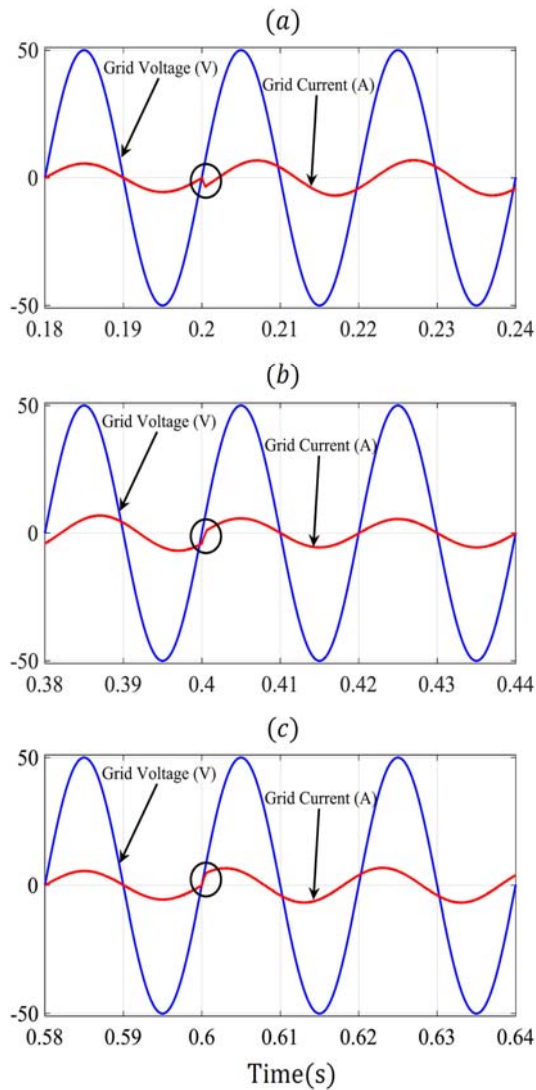
Fig. 13. Grid current and voltage angle change under reactive power change.

4. CONCLUSIONS

In this paper, an improved control scheme based on predictive control strategy for three phase dual-stage grid tied photovoltaic (PV) system was presented. A predictive current control technique, VS-INC/PCC, is proposed and applied to the first stage in order to track the MPP quickly and accurately. Whereas, VOC based on predictive control strategy through SVM, PS-VOC, was employed to control the second stage in order to inject the generated PV power in addition to the reactive power demanded by the grid operator with high grid currents quality. The simulation results clearly show a significant enhancement by applying the proposed MPPT method in comparison with the conventional INC and INC through PCC methods in terms of accuracy tracking, response time and stability around the maximum power point under irradiation changes. Moreover, the proposed PS-VOC control of grid tied two-level inverter presents high grid current quality in accordance with international standards (IEEE-519) for any irradiation and reactive power changes.

NOMENCLATURE

$i_{pv}(k)$	Measured PV array current (A)
$i_{pv}(k-1)$	Previous measured PV array current (A)
$v_{pv}(k)$	Measured PV array voltage (V)
$v_{pv}(k-1)$	Previous measured PV array voltage (V)
$p_{pv}(k)$	Measured PV array power (W)
$\Delta p_{pv}(k)$	Measured PV array power variation (W)
$\Delta i_{pv}(k)$	Measured PV array current variation (A)
$\Delta v_{pv}(k)$	Measured PV array voltage variation (V)
$i_{ref}(k)$	Reference PV array current (A)
$i_{ref}(k-1)$	Previous reference PV array current (A)
$\Delta i_{ref}(k)$	Step of reference PV array current (A)
$d(k), d(k+1)$	Actual and predicted duty cycle
G	Irradiance (W/m²)
$i_{inv}(k)$	Inverter input current (A)
S	Control action of boost converter
$v_{dc}(h), v_{dc\_ref}(h)$	Measured DC-link voltage & reference DC-link voltage (V)
$e_{ga}(h), e_{gb}(h), e_{gc}(h)$	Grid voltages (V)
$e_{gd}(h), e_{gq}(h)$	Grid voltages in d-q frame
$i_{ga}(h), i_{gb}(h), i_{gc}(h)$	Grid currents (A)
$i_d(h), i_q(h)$	Measured grid current in d-q frame
$i_d(h+1), i_q(h+1)$	Predicted grid current in d-q frame

$i_{d\_ref}(h), i_{q\_ref}(h)$	Reference grid current in d_q frame
$i_{d\_ref}(h+1), i_{q\_ref}(h+1)$	Predicted reference grid current in d_q frame
$v_\alpha(h), v_\beta(h)$	Voltage vector in α-β frame
$v_d(h), v_q(h)$	Voltage vector in d-q frame
$Q_{ref}(h)$	Reactive power reference (VAR)
ω_g	Grid angular frequency
θ	Angle
$S_{a1}, S_{a2}, S_{b1}, S_{b2}, S_{c1}, S_{c2}$	Control action of the inverter
MPPT	Maximum power point tracking
MPPT P&O	MPPT Perturb and observe
MPPT INC	MPPT Incremental conductance
SVM	Space vector modulation
DPC	Direct power control
V-DPC	Voltage based direct power control
VFOC	Voltage flux-oriented control
PLL	Phase Locked Loop
VS-INC	Variable step-size incremental conductance
PCC	Predictive current control
VOC	Voltage oriented control
PS-VOC	VOC based on predictive control strategy and SVM
THD	Total harmonic distortion
PI	Proportional-Integral controller
PWM	Pulse width modulation

REFERENCES

Ahmed, M. E. S., Orabi, M., AbdelRahim, O. M. (2013). Two-stage micro-grid inverter with high-voltage gain for photovoltaic applications.*IET Power Electronics*, 6(9), 1812-1821.

Algazar, M. M., El-Halim, H. A., Salem, M. E. E. K. (2012). Maximum power point tracking using fuzzy logic control.*Electrical Power and Energy Systems*, 39(1), 21–28.

Azzouzi M., (2013). Optimization of Photovoltaic Generator by Using P&O Algorithm Under Different Weather Conditions. *Journal of Control Engineering and Applied Informatics,* 15(2), 12-19.

Bendib, B., Belmili, H., Krim, F. (2015). A survey of the most used MPPT methods: Conventional and advanced algorithms applied for photovoltaic systems, *Renewable and Sustainable Energy Reviews,* 45, 637-648.

Bianconi, E., Calvente, J., Giral, R., Mamarelis, E., Petrone, G., Ramos-Paja, C. A., Spagnuolo G., Vitelli, M. (2013). A fast current-based MPPT technique employing sliding mode control.*IEEE Transactions on Industrial Electronics*, 60(3), 1168-1178.

Boumaaraf, H., Talha, A., Bouhali, O. (2015). A three-phase NPC grid-connected inverter for photovoltaic applications using neural network MPPT.*Renewable and Sustainable Energy Reviews,* 49, 1171-1179.

Bratcu, A. I., Munteanu, I., Bacha, S., Raison, B. (2008). Maximum Power Point Tracking of Grid-connected Photovoltaic Arrays by Using Extremum Seeking Control. *Journal of Control Engineering and Applied Informatics,* 10(4), 3-12.

Chen, L., Amirahmadi, A., Zhang, Q., Kutkut, N., Batarseh, I. (2014). Design and implementation of three-phase two-stage grid-connected module integrated converter.*IEEE Transactions on Power Electronics,* 29(8), 3881-3892.

de Oliveira, F. M., da Silva, S. A. O., Durand, F. R., Sampaio, L. P., Bacon, V. D., Campanhol, L. B. (2016). Grid-tied photovoltaic system based on PSO MPPT technique with active power line conditioning.*IET Power Electronics,* 9(6), 1180-1191.

Feroura, H., Krim, F., Tabli, B., Laib, A. (2017a). Finite-set model predictive voltage control for islanded three phase current source inverter.*IEEE 5th International Conference on Electrical Engineering (ICEE-B),* 29-31 Oct, Boumerdes, Algeria, pp. 1-5.

Feroura, H., Krim, F., Talbi, B., Laib, A., Belaout, A. (2017b). Finite-Set Model Predictive Direct Power Control of Grid Connected Current Source Inverter. *ElektronikairElektrotechnika,* 23(5), 36-40.

Harrag,A., Messalti,S. (2015). Variable step size modified P&O MPPT algorithm using GA-based hybrid offline/online PID controller.*Renewable and Sustainable Energy Reviews*, 49, 1247-1260.

Hu, J., Zhu, Z. Q. (2011). Investigation on Switching Patterns of Direct Power Control Strategies for Grid-Connected DC–AC Converters Based on Power Variation Rates.*IEEE Transactions on Power Electronics,* 26(12), 3582-3598.

Jain, C., Singh, B. (2017). A Three-Phase Grid Tied SPV System with Adaptive DC Link Voltage for CPI Voltage Variations.*IEEE Transactions on Sustainable Energy,* 7(1), 337-344.

Kakosimos, P. E., Kladas, A. G. (2011). Implementation of photovoltaic array MPPT through fixed step predictive control technique.*Renewable Energy,* 36(9), 2508-2514.

Kakosimos, P. E., Kladas, A. G., Manias, S. N. (2013). Fast photovoltaic-system voltage-or current-oriented MPPT employing a predictive digital current-controlled converter.*IEEE Transactions on Industrial Electronics,* 60(12), 5673-5685.

Kihel, A., Krim, F., Laib, A. (2017). MPPT voltage-oriented loop based on integral sliding mode control applied to the boost converter. *IEEE 6th International Conference on Systems and Control (ICSC),*7-9 May, Batna, Algeria, pp. 205-209.

Kollimalla, S. K., Mishra, M. K. (2014). A Novel Adaptive P&O MPPT Algorithm Considering Sudden Changes in the Irradiance.*IEEE Transactions on Energy Conversion*, 29(3), 602-610.

Liu, F., Duan, S., Liu, F., Liu, B., Kang, Y. (2008). A Variable Step Size INC MPPT Method for PV Systems.*IEEE Transactions on Industrial Electronics,* 55(7), 2622-2628.

Loukriz, A.,Haddadi M.,Messalti,S. (2016).Simulation and experimental design of a new advanced variable step size Incremental Conductance MPPT algorithm for PV systems.*ISA transactions*, 62, 30-38.

Malinowski, M., Jasinski, M., Kazmierkowski, M. P. (2004). Simple Direct Power Control of Three-Phase PWM Rectifier Using Space-Vector Modulation (DPC-SVM). *IEEE Transactions on Industrial Electronics*, 51(2), 447-454.

Malinowski, M., Kazmierkowski, M. P., Hansen, S., Blaabjerg, F., Marques, G. D. (2001). Virtual Flux Based Direct Power Control of Three-phase PWM Rectifiers, *IEEE Transactions on industry applications,* 37(4), 1019-1027.

Menadi,A., Abdeddaim,S., Ghamri,A., Betka, A. (2015). Implementation of fuzzy-sliding mode-based control of a grid connected photovoltaic system. *ISA transactions*, 58, 586-594.

Pradhan, R.,Subudhi, B.(2016). Double Integral Sliding Mode MPPT Control of a Photovoltaic System.*IEEE Transactions on Control Systems Technology*, 24(1), 285-292.

Petcut, F. M., Leonida-Dragomir, T. (2010). Solar cell parameter identification using genetic algorithms. *Journal of Control Engineering and Applied Informatics*, 12(1), 30-37.

Radjai, T., Rahmani, L., Mekhilef, S., Gaubert, J. P. (2014). Implementation of a modified incremental conductance MPPT algorithm with direct control based on a fuzzy duty cycle change estimator using dSPACE.*Solar Energy*, 110, 325–337.

Rodriguez, J., Pontt, J., Silva, C. A., Correa, P., Lezana, P., Cortés, P., Ammann, U. (2007). Predictive current control of a voltage source inverter.*IEEE Transactions on Industrial Electronics*, 54(1), 495-503.

Safari, A., Mekhilef, S. (2011). Simulation and Hardware Implementation of Incremental Conductance MPPT with Direct Control Method Using Cuk Converter.*IEEE Transactions on Industrial Electronics*, 58(4), 1154-1161.

Talbi, B., Krim, F., Rekioua, T., Laib, A.,Feroura, H. (2017). Design and hardware validation of modified P&O algorithm by fuzzy logic approach based on model predictive control for MPPT of PV systems. *Journal of Renewable and Sustainable Energy*, 9(4), 043503.

Talbi, B., Krim, F., Rekioua, T., Mekhilef, S., Laib, A., Belaout, A. (2018). A high-performance control scheme for photovoltaic pumping system under sudden irradiance and load changes. *Solar Energy*, 159, 353-368.

Teodorescu, R., Liserre, M., Rodriguez, P. (2011). Grid converters for photovoltaic and wind power systems. *John Wiley & Sons*.

Van Dijk, E., Spruijt, J. N., O'sullivan, D. M., Klaassens, J. B. (1995). PWM-switch modeling of DC-DC converters.*IEEE Transactions on Power Electronics,* 10(6), 659-665.

Wai, R. J., Wang, W. H., Lin, C. Y. (2008). High-Performance Stand-Alone Photovoltaic Generation System.*IEEE Transactions on Industrial Electronics,* 55(1), 240–250.

Yaramasu, V., Wu, B., Chen, J. Chen (2014). Model-Predictive Control of Grid-Tied Four-Level Diode-Clamped Inverters for High-Power Wind Energy Conversion Systems.*IEEE Transactions on Power Electronics*, 29(6), 2861-2873.

Zainuri, M. A. A. M., Radzi, M. A. M., Soh, A. C., Rahim, N. A. (2013). Development of adaptive perturb and observe-fuzzy control maximum power point tracking for photovoltaic boost dc–dc converter.*IET Renewable Power Generation*, 8(2), 183–194.